The Cosmological Constant is Back

Lawrence M. Krauss and Michael S. Turner (1995)

- If the Universe possesses a nonzero cosmological constant, Λ, that corresponds to the energy density of the vacuum

- Einstein thought Λ necessary to obtain static models of Universe

- Steady State (Bondi, Gold, and Hoyle)
  - use Λ to resolve the age of the Universe crisis
  - use Λ to construct a universe satisfying the “Perfect Cosmological Principle”

Inflation

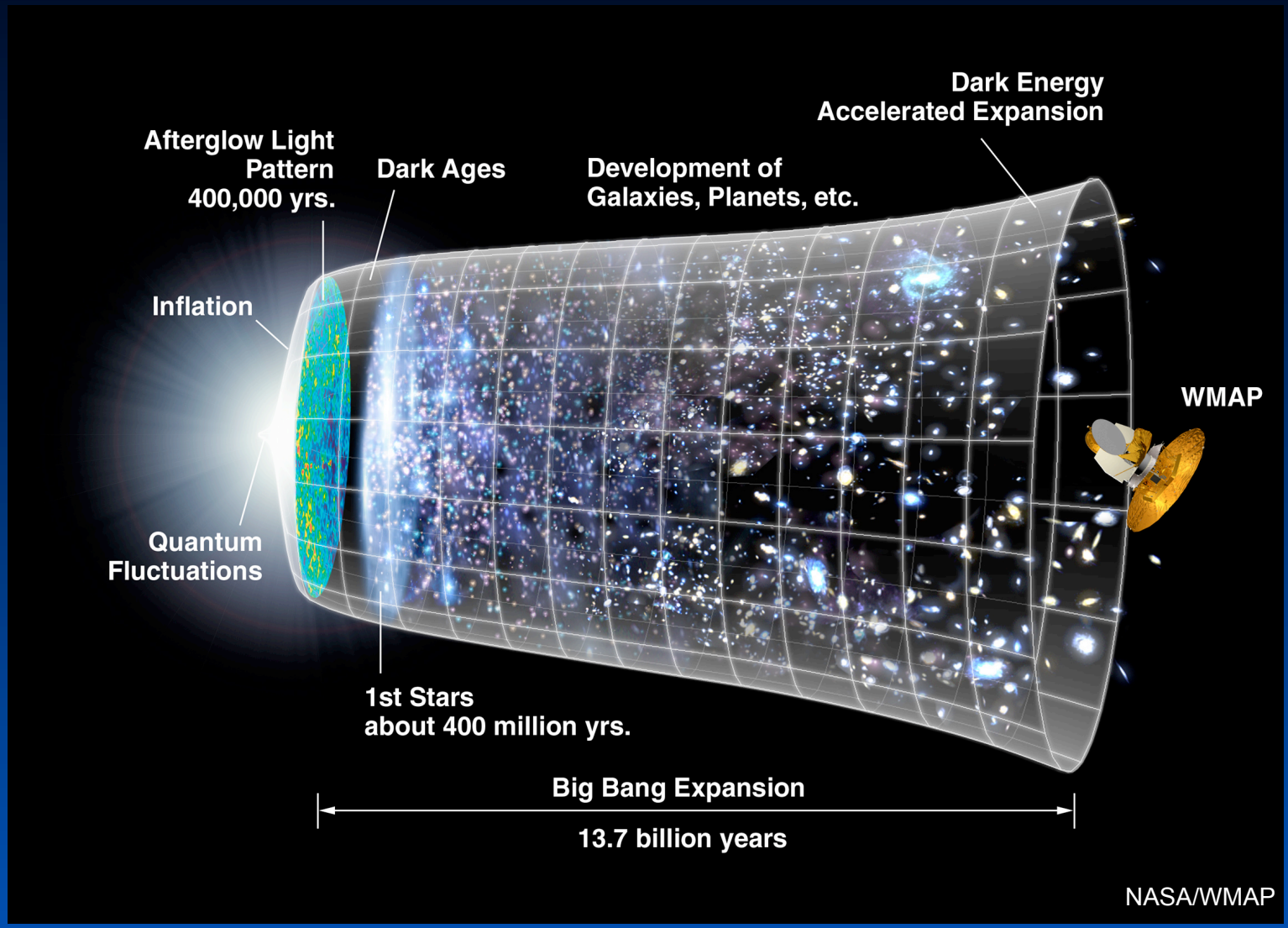
Dark Energy
Accelerated Expansion
Afterglow Light
Pattern
400,000 yrs.
Dark Ages
Development of
Galaxies, Planets, etc.
Inflation
WMAP
Quantum
Fluctuations
1st Stars
about 400 million yrs.
Big Bang Expansion
13.7 billion years
NASA/WMAP

Motivation for a Cosmological Constant

- Age of the Universe
- Formation Structure
- Mass Density

Constraints on Ω_M in a Flat Universe vs H_0

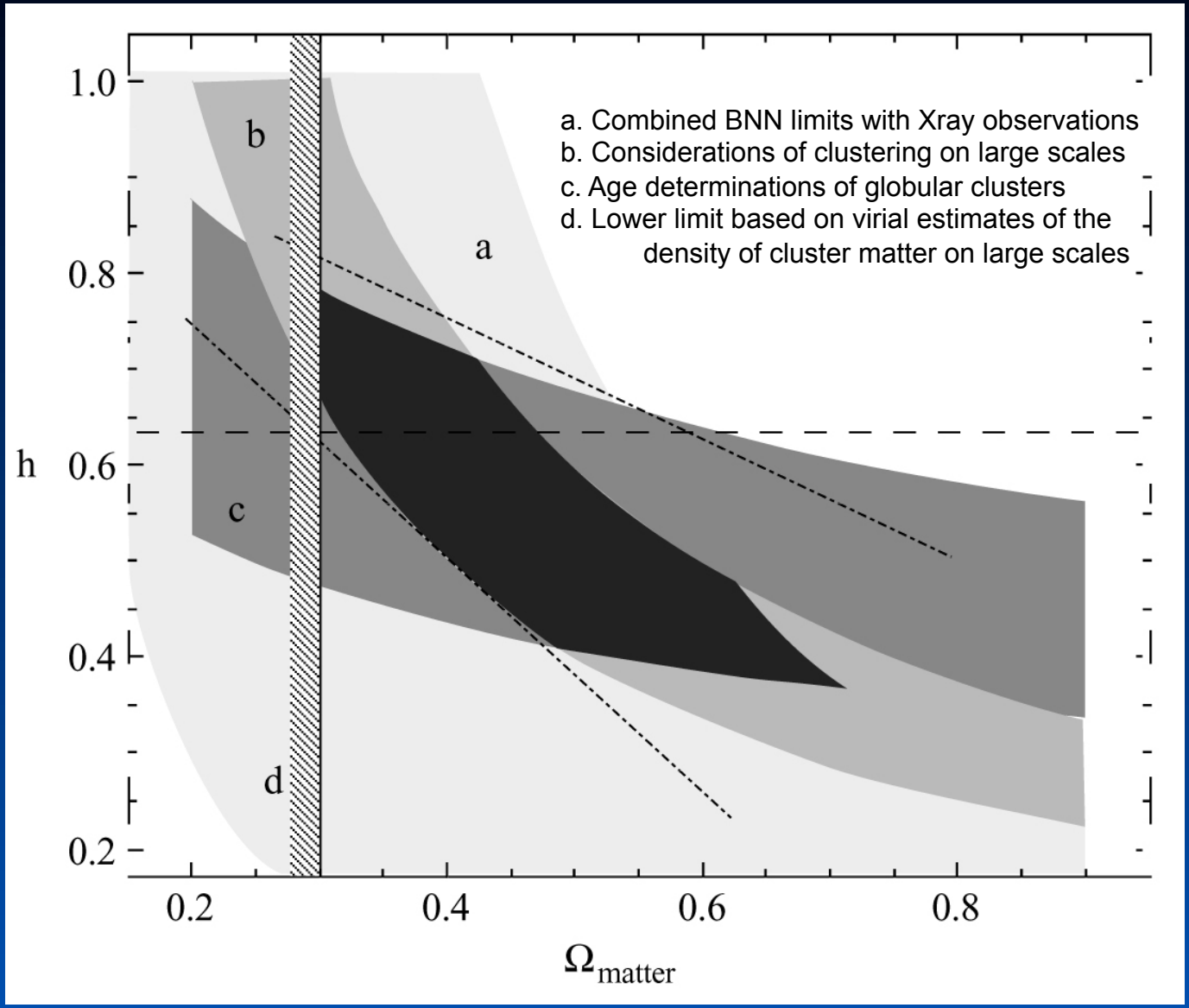

Fundamental Concerns

- Λ implies a special epoch at z=0 where its role in the dynamics of the Universe becomes dominant
- A nonzero Λ corresponds to vacuum energy density
- Particle theorists have yet to successfully constrain the value of Λ

Observational Evidence from Supernovae for an Accelerating Universe and a Cosmological Constant

Riess et al. (1998)
High-z Supernova Search Team

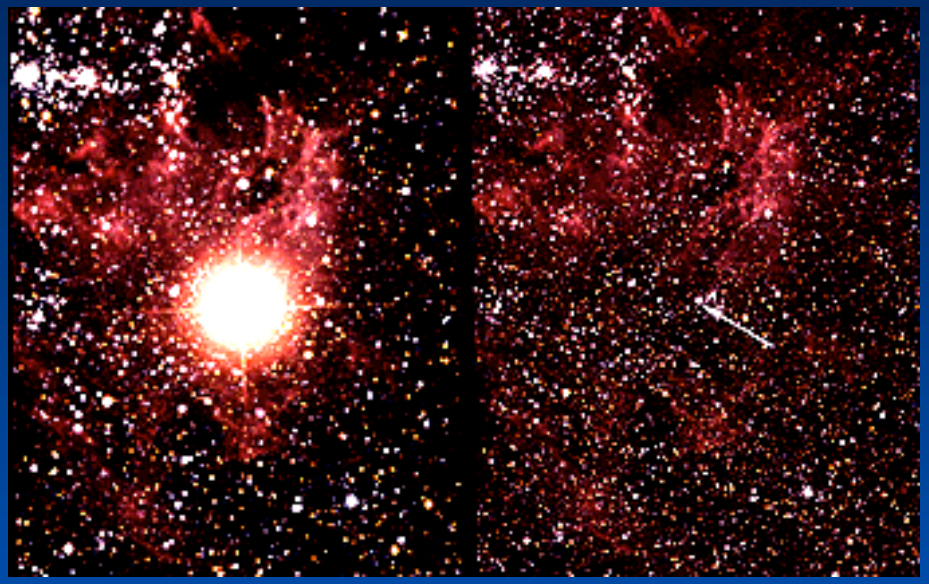

SN 1987A “After” and “Before.” Photo credit: NASA

In order to determine the history of the Universe, need to measure expansion factor of the Universe, a(t), and coordinate radial distance r(t)

- a, r, and t are not directly measurable

Instead, we can measure:

- Redshift $z(t) = a_0/a(t) - 1$
- Luminosity Distance $D_L = (L/4\pi F)^{1/2}$

Type Ia Supernovae

- Results from violent explosion of white dwarf star
- Accretes mass from a binary companion

- As the mass approaches the Chandrasekhar limit, runaway thermonuclear reactions occur

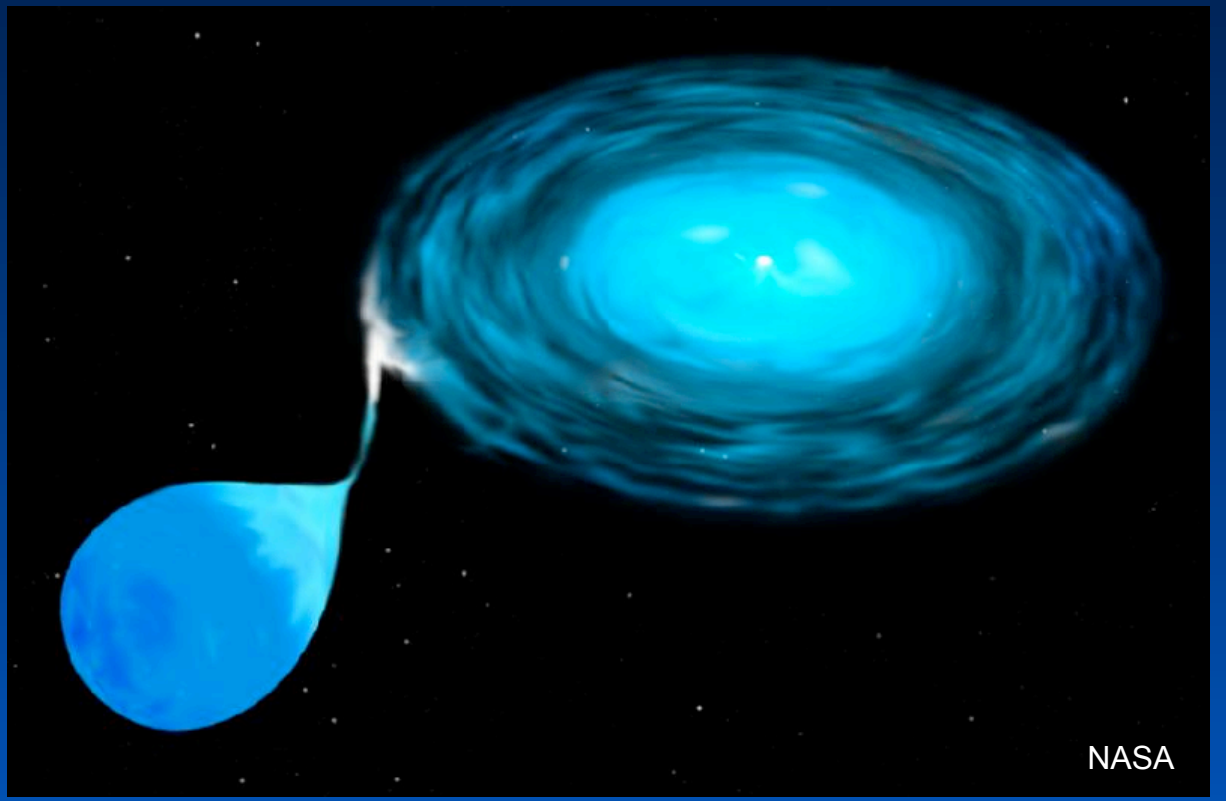

Overview

- First evidence of dark energy
- Type Ia Supernovae are homogeneous and bright
- 16 high redshift and 22 lower redshift SNe Ia are observed
- Redshift range $0.3 < z < 0.6$

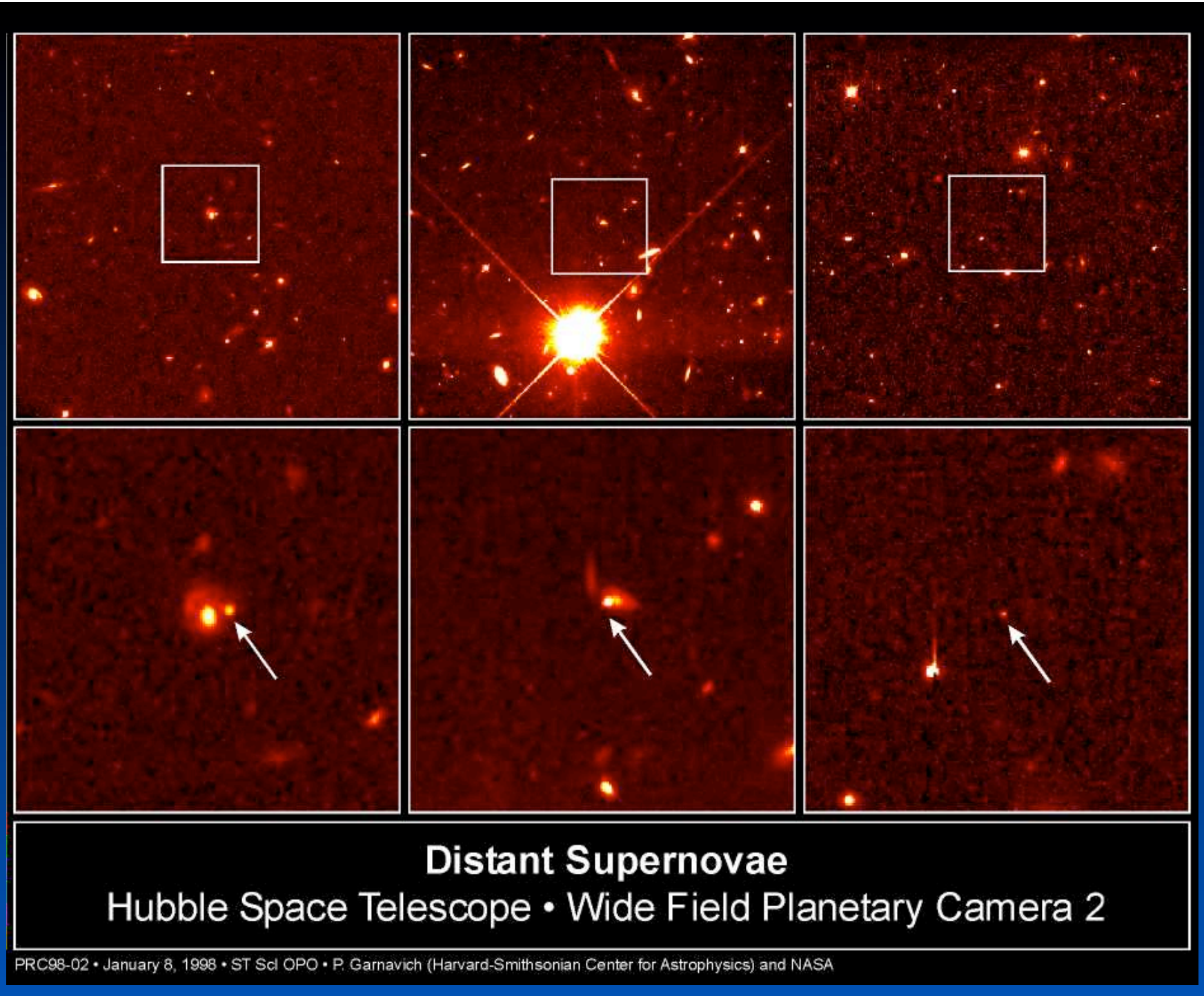

Distant Supernovae

Hubble Space Telescope • Wide Field Planetary Camera 2

PRC98-02 • January 8, 1998 • ST ScI OPO • P. Garnavich (Harvard-Smithsonian Center for Astrophysics) and NASA

Identification Spectra of high-z SNe Ia

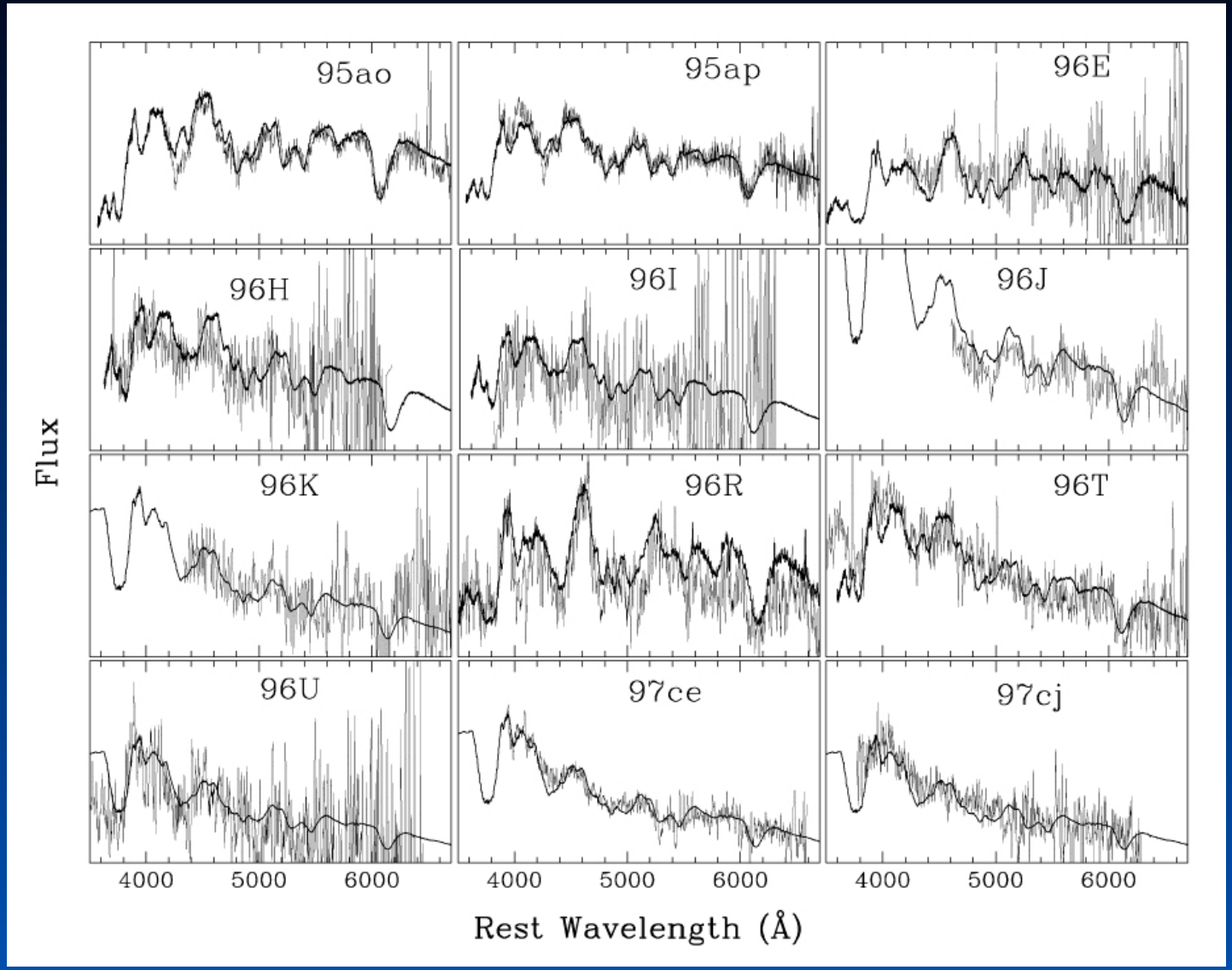

Light Curve Fitting

Requirements:

- a date of maximum (t)
- a light curve width parameter (Δ)
- a distance modulus (μ_B)
- an extinction by dust (A_B)

$\mu_B = 5 \log D_L + 25$

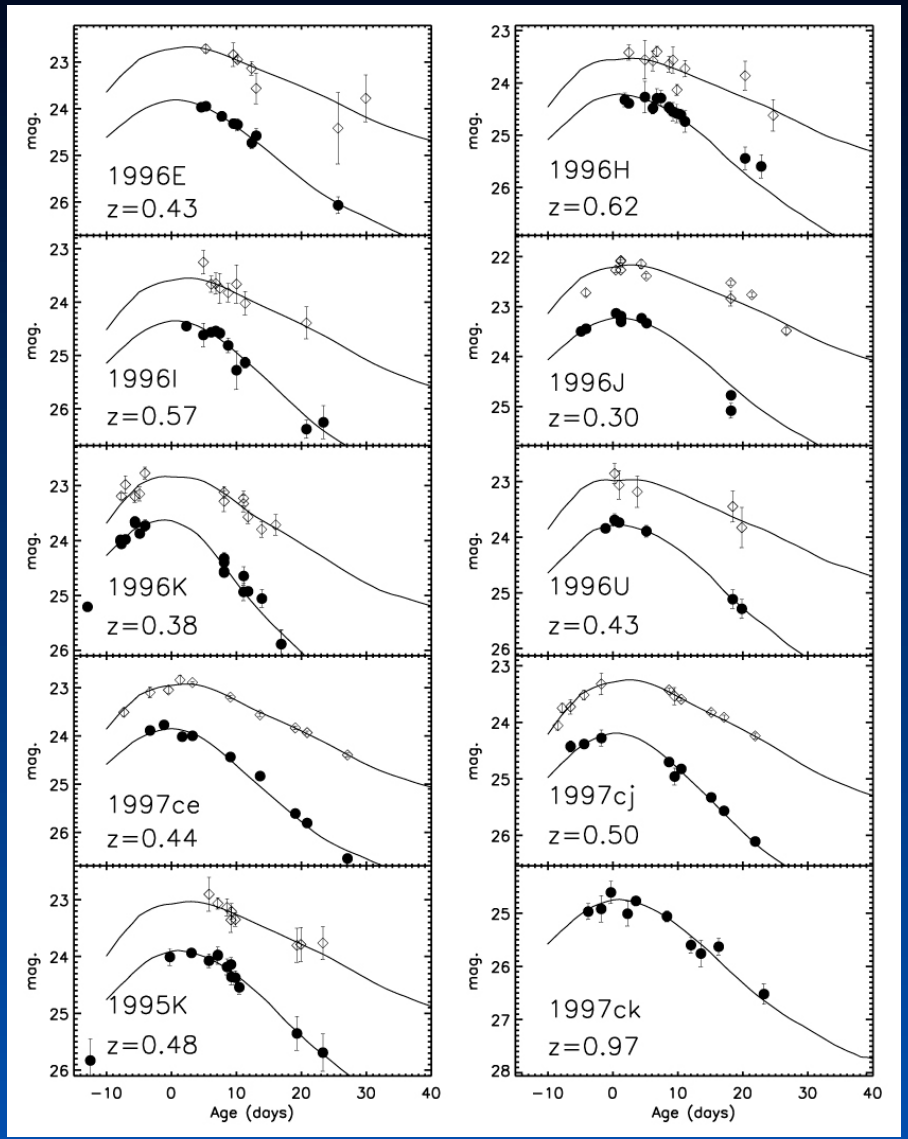

Luminosity Distance

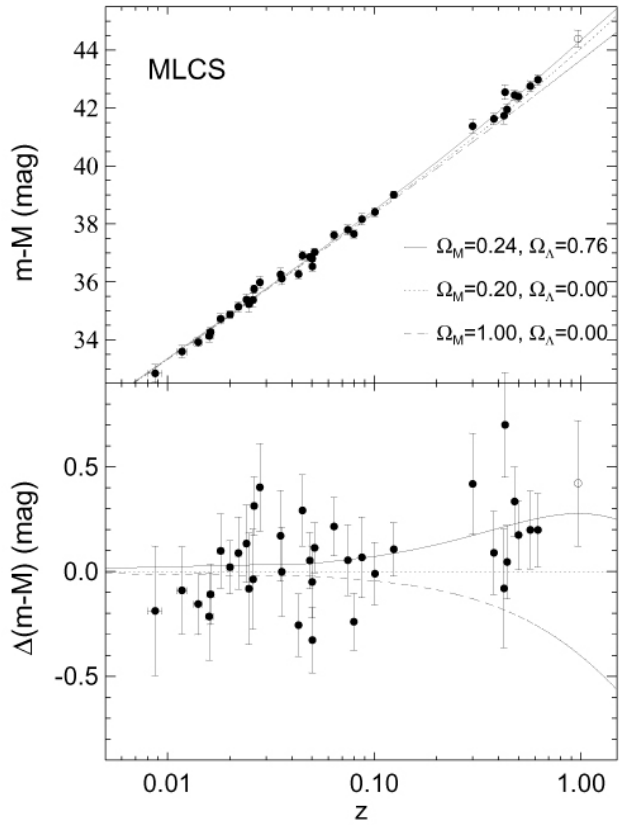

FIG. 4.—MLCS SNe Ia Hubble diagram. The upper panel shows the Hubble diagram for the low-redshift and high-redshift SNe Ia samples with distances measured from the MLCS method (Riess et al. 1995, 1996a; Appendix of this paper). Overplotted are three cosmologies: "low" and "high" Ω_M with $\Omega_\Lambda = 0$ and the best fit for a flat cosmology, $\Omega_M = 0.24$, $\Omega_\Lambda = 0.76$. The bottom panel shows the difference between data and models with $\Omega_M = 0.20$, $\Omega_\Lambda = 0$. The open symbol is SN 1997ck ($z = 0.97$), which lacks spectroscopic classification and a color measurement. The average difference between the data and the $\Omega_M = 0.20$, $\Omega_\Lambda = 0$ prediction is 0.25 mag.

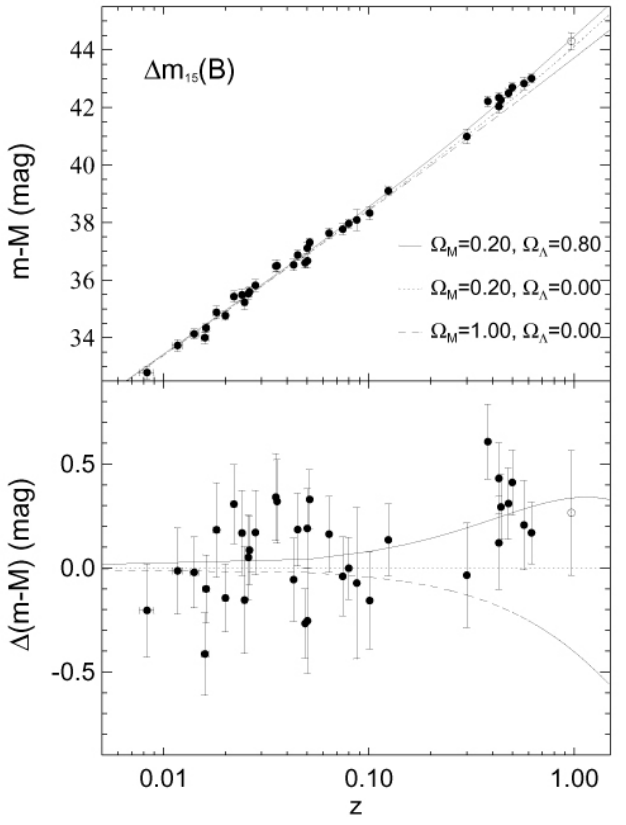

FIG. 5.—$\Delta m_{15}(B)$ SN Ia Hubble diagram. The upper panel shows the Hubble diagram for the low-redshift and high-redshift SNe Ia samples with distances measured from the template-fitting method parameterized by $\Delta m_{15}(B)$ (Hamuy et al. 1995, 1996d). Overplotted are three cosmologies: "low" and "high" Ω_M with $\Omega_\Lambda = 0$ and the best fit for a flat cosmology, $\Omega_M = 0.20$, $\Omega_\Lambda = 0.80$. The bottom panel shows the difference between data and models from the $\Omega_M = 0.20$, $\Omega_\Lambda = 0$ prediction. The open symbol is SN 1997ck ($z = 0.97$), which lacks spectroscopic classification and a color measurement. The average difference between the data and the $\Omega_M = 0.20$, $\Omega_\Lambda = 0$ prediction is 0.28 mag.

$$D_L = \left(\frac{L}{4\pi F}\right)^{1/2}$$

$$D_L = cH_0^{-1}(1+z)\,|\Omega_k|^{-1/2}\, sinn\{|\Omega_k|^{1/2}\int_0^z dz[(1+z)^2(1+\Omega_M z) - z(2+z)\Omega_\Lambda]^{-1/2}\},$$

Luminosity Distance

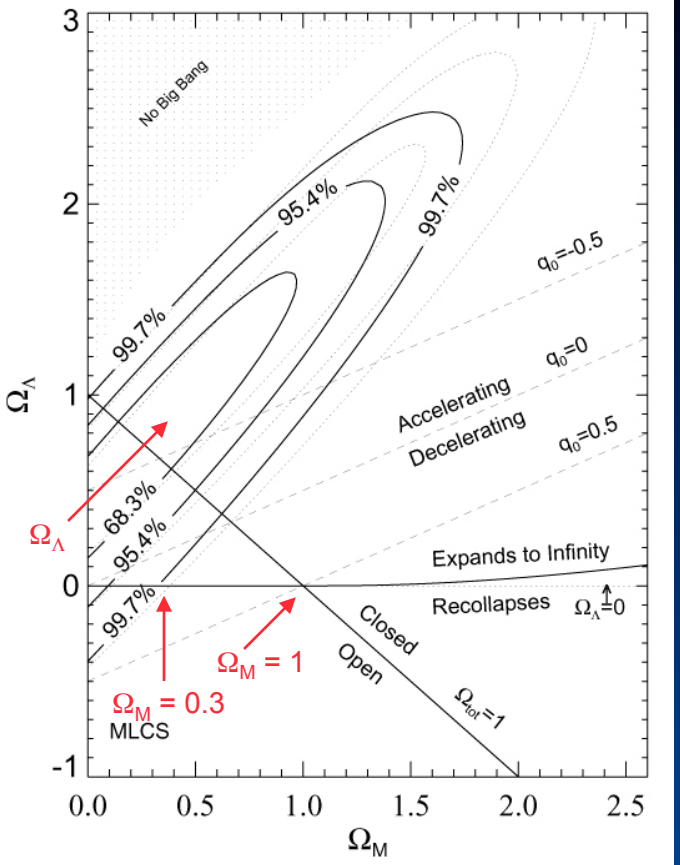

FIG. 6.—Joint confidence intervals for $(\Omega_M, \Omega_\Lambda)$ from SNe Ia. The solid contours are results from the MLCS method applied to well-observed SNe Ia light curves together with the snapshot method (Riess et al. 1998b) applied to incomplete SNe Ia light curves. The dotted contours are for the same objects excluding the unclassified SN 1997ck ($z = 0.97$). Regions representing specific cosmological scenarios are illustrated. Contours are closed by their intersection with the line $\Omega_M = 0$.

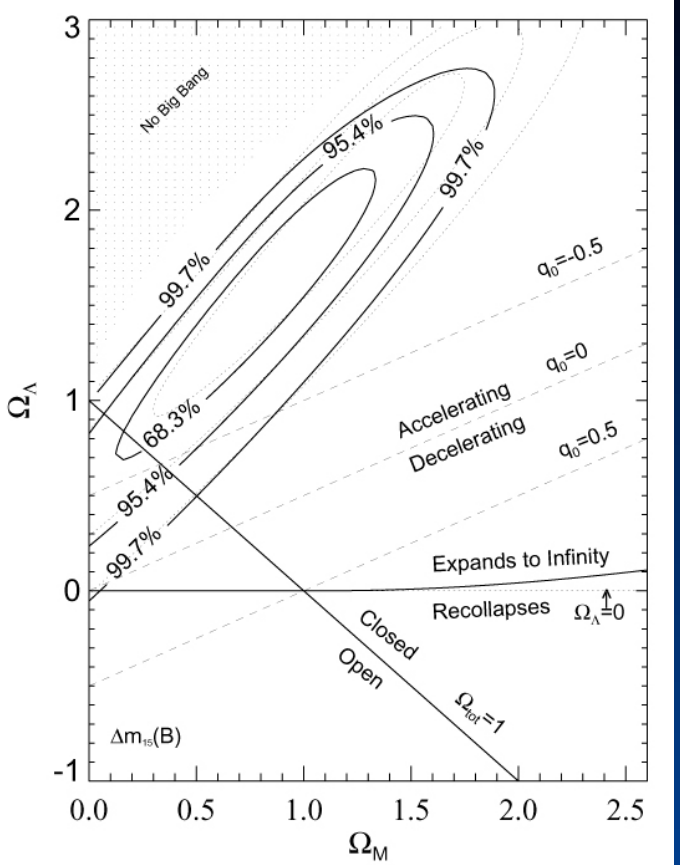

FIG. 7.—Joint confidence intervals for $(\Omega_M, \Omega_\Lambda)$ from SNe Ia. The solid contours are results from the template-fitting method applied to well-observed SNe Ia light curves together with the snapshot method (Riess et al. 1998b) applied to incomplete SNe Ia light curves. The dotted contours are for the same objects excluding the unclassified SN 1997ck ($z = 0.97$). Regions representing specific cosmological scenarios are illustrated. Contours are closed by their intersection with the line $\Omega_M = 0$.

$$\chi^2(H_0, \Omega_M, \Omega_\Lambda) = \sum_i \frac{\left(\mu_{p,i}(z_i; H_0, \Omega_M, \Omega_\Lambda) - \mu_{0,i}\right)^2}{\sigma^2_{\mu_0,i} + \sigma^2_v}$$

Deceleration Parameter q_0

TABLE 8

COSMOLOGICAL RESULTS

METHOD (HIGH-z SNe)	NO CONSTRAINT[a] H_0	Ω_M	Ω_Λ	χ^2_ν	t_0	$p(\Omega_\Lambda \geq 0)$	$p(q_0 \leq 0)$	q_0	$\Omega_{tot} \equiv 1$ Ω_M	$\Omega_\Lambda \equiv 0$ Ω_M	$\Omega_M \equiv 0.2$ Ω_Λ
MLCS + Snapshot (15)[b]	...	...	...	1.19	...	99.7% (3.0 σ)	99.5% (2.8 σ)	-0.98 ± 0.40	0.28 ± 0.10	-0.34 ± 0.21	0.65 ± 0.22
ΔM_{15} + Snapshot (15)[b]	...	...	...	1.03	...	>99.9% (4.0 σ)	>99.9% (3.9 σ)	-1.34 ± 0.40	0.17 ± 0.09	-0.48 ± 0.19	0.84 ± 0.18
MLCS + Snap. + 97ck (16)	...	$0.24^{+0.56}_{-0.24}$	$0.72^{+0.72}_{-0.48}$	1.17	...	99.5% (2.8 σ)	99.3% (2.7 σ)	-0.75 ± 0.32	0.24 ± 0.10	-0.35 ± 0.18	0.66 ± 0.21
ΔM_{15} + Snap. + 97ck (16)	...	$0.80^{+0.40}_{-0.48}$	$1.56^{+0.52}_{-0.70}$	1.04	...	>99.9% (3.9 σ)	>99.9% (3.8 σ)	-1.14 ± 0.30	0.21 ± 0.09	-0.41 ± 0.17	0.80 ± 0.19
MLCS (9)	65.2 ± 1.3[c]	...	...	1.19	$13.6^{+1.0}_{-0.8}$	99.6% (2.9 σ)	99.4% (2.4 σ)	-0.92 ± 0.42	0.28 ± 0.10	-0.38 ± 0.22	0.68 ± 0.24
ΔM_{15} (9)	63.8 ± 1.3[c]	...	...	1.05	$14.8^{+1.0}_{-0.8}$	>99.9% (3.9 σ)	>99.9% (3.8 σ)	-1.38 ± 0.46	0.16 ± 0.09	-0.52 ± 0.20	0.88 ± 0.19
MLCS + 97ck (10)	65.2 ± 1.3[c]	$0.00^{+0.60}_{-0.00}$	$0.48^{+0.72}_{-0.24}$	1.17	$14.2^{+1.3}_{-1.0}$	99.5% (2.8 σ)	99.3% (2.7 σ)	-0.74 ± 0.32	0.24 ± 0.10	-0.38 ± 0.19	0.68 ± 0.22
ΔM_{15} + 97ck (10)	63.7 ± 1.3[c]	$0.72^{+0.44}_{-0.56}$	$1.48^{+0.56}_{-0.68}$	1.04	$15.1^{+1.1}_{-0.9}$	>99.9% (3.8 σ)	>99.9% (3.7 σ)	-1.11 ± 0.32	0.20 ± 0.09	-0.44 ± 0.18	0.84 ± 0.20
Snapshot (6)	63.4 ± 2.7[c]	...	...	1.30	...	89.1% (1.6 σ)	78.9% (1.3 σ)	-0.70 ± 0.80	0.40 ± 0.50	0.06 ± 0.70	0.44 ± 0.60

[a] $\Omega_M \geq 0$.
[b] Complete set of spectroscopic SNe Ia.
[c] This uncertainty reflects only the statistical error from the variance of SNe Ia in the Hubble flow. It does not include any contribution from the (much larger) SN Ia absolute magnitude error.

$$q_0 = \frac{\Omega_M}{2} - \Omega_\Lambda$$

Dynamical Age of the Universe

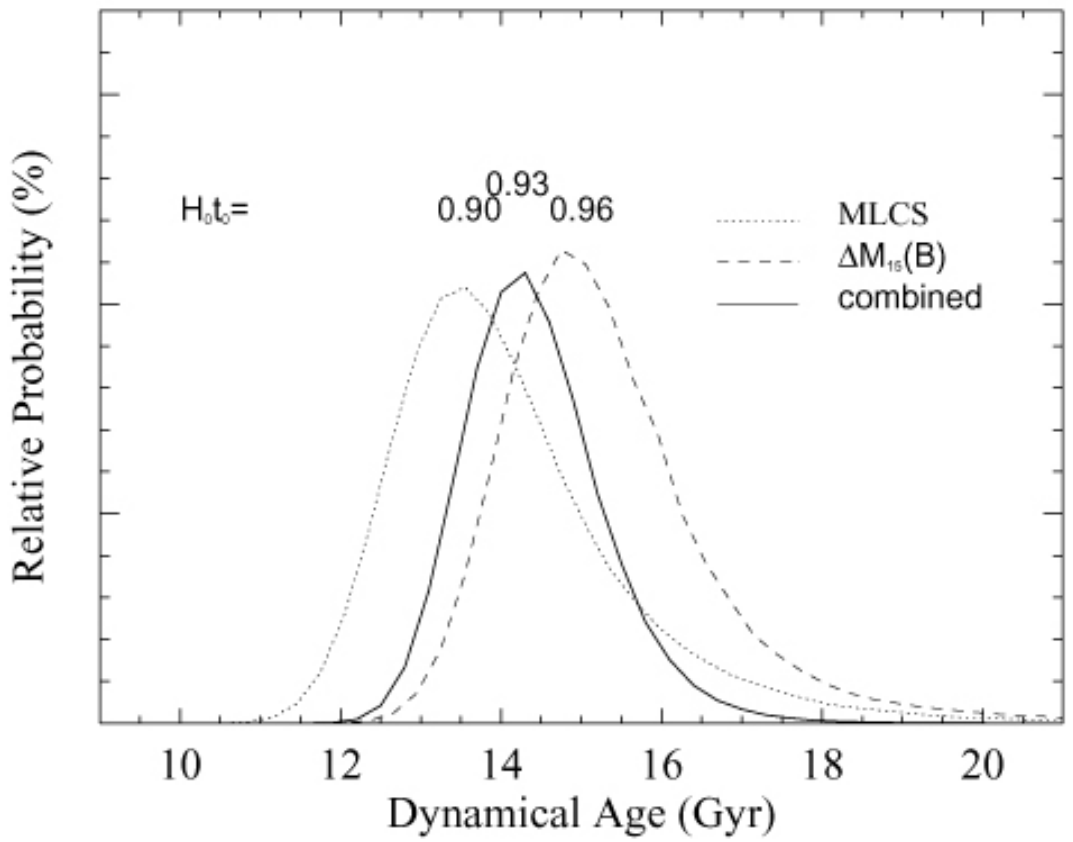

FIG. 8.—PDF for the dynamical age of the universe from SNe Ia (eq. [19]). The PDF for the dynamical age derived from the PDFs for H_0, Ω_M, Ω_Λ is shown for the two different distance methods without the unclassified SN 1997ck. A naive average (see § 4.2) yields an estimate of $14.2^{+1.0}_{-0.8}$ Gyr, not including the systematic uncertainties in the Cepheid distance scale.

Dynamical Age of the Universe

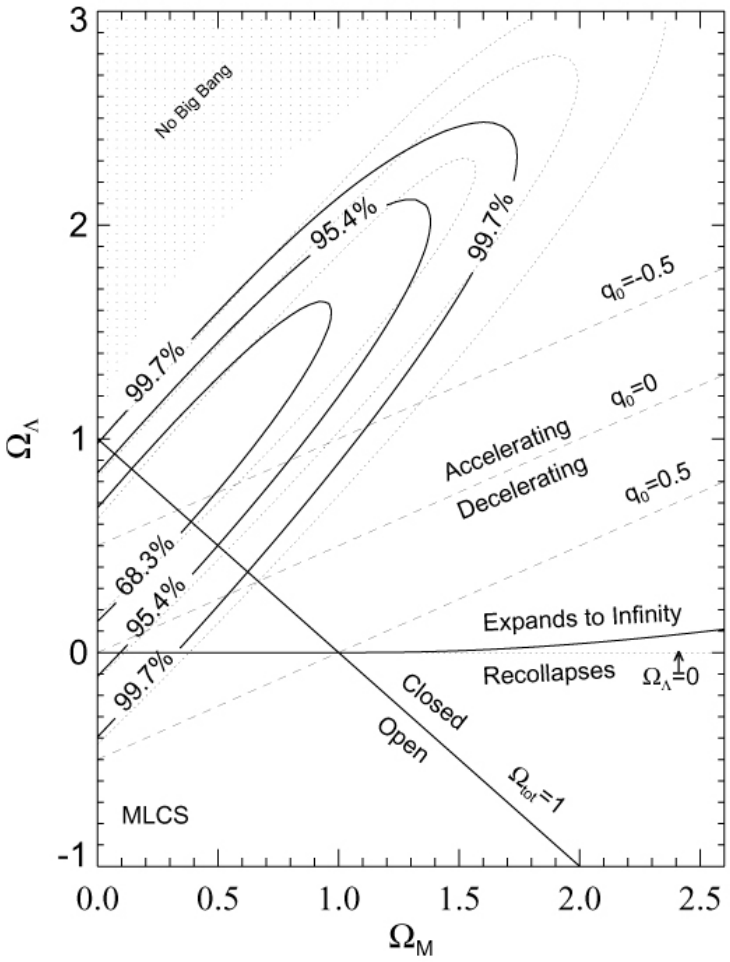

FIG. 6.—Joint confidence intervals for $(\Omega_M, \Omega_\Lambda)$ from SNe Ia. The solid contours are results from the MLCS method applied to well-observed SNe Ia light curves together with the snapshot method (Riess et al. 1998b) applied to incomplete SNe Ia light curves. The dotted contours are for the same objects excluding the unclassified SN 1997ck ($z = 0.97$). Regions representing specific cosmological scenarios are illustrated. Contours are closed by their intersection with the line $\Omega_M = 0$.

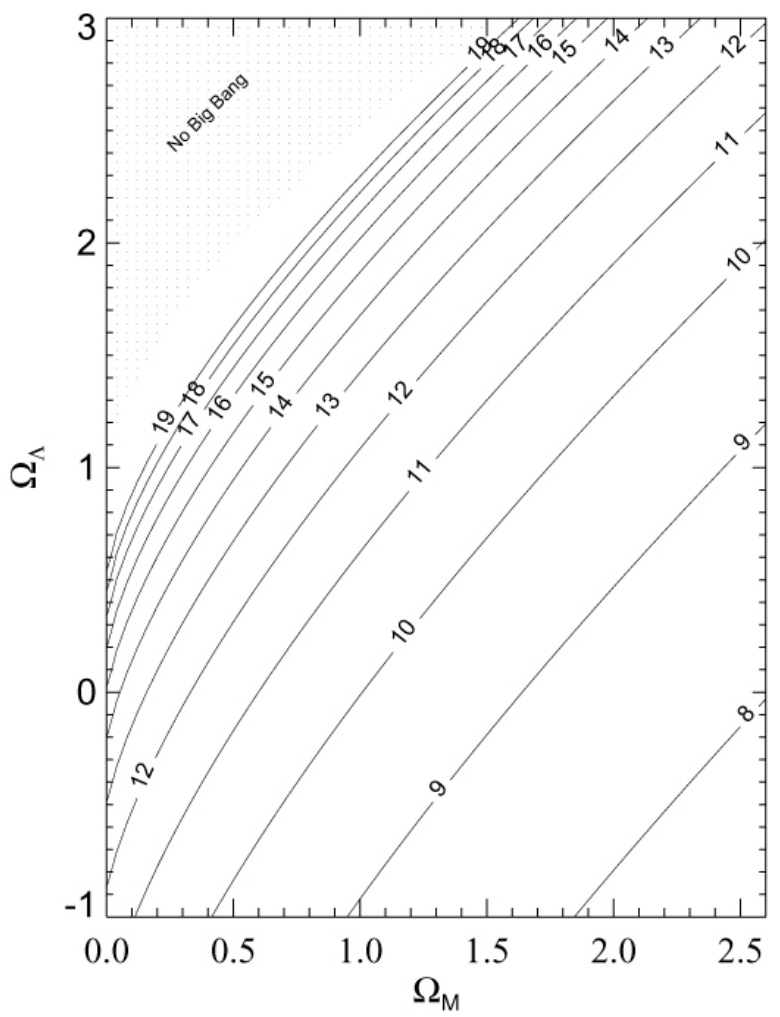

FIG. 9.—Lines of constant dynamical age in Gyr in the $(\Omega_M, \Omega_\Lambda)$-plane. Comparing these lines with the error ellipses in Figs. 5 and 7 reveals the leverage this experiment has on measuring the dynamical age. This plot assumes $H_0 = 65$ km s^{-1} Mpc^{-1} as determined from nearby SNe Ia and is subject to the zero point of the Cepheid distance scale.

Uncertainties

- Evolution
- Grey Extinction
- Sample Selection Bias
- A Local Void
- Weak Gravitational Lensing
- Sample Contamination

Evolution

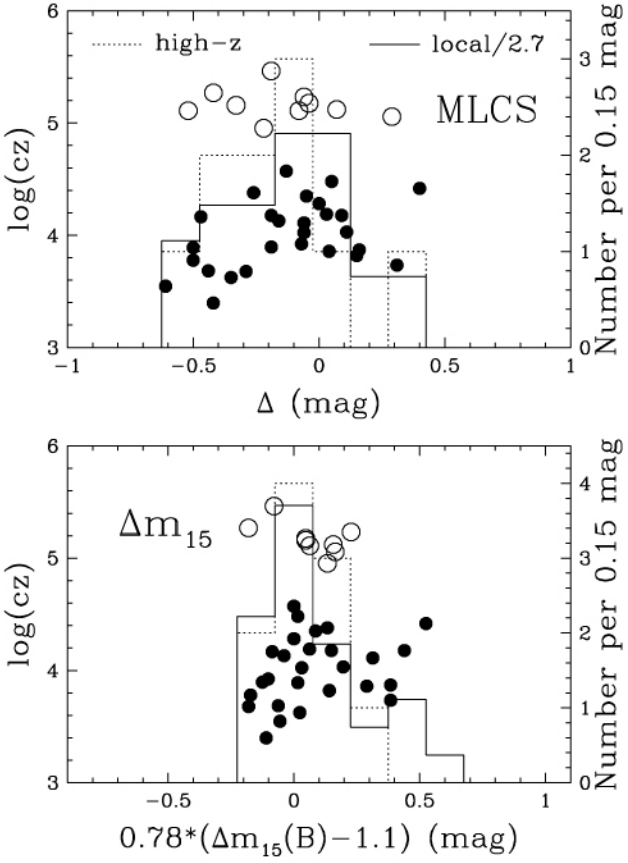

FIG. 10.—Distributions of MLCS light curve shape parameters, Δ, and template-fitting parameters, $\Delta m_{15}(B)$, for the high- and low-redshift samples of SNe Ia. Positive values for Δ and $\Delta m_{15}(B) > 1.1$ correspond to intrinsically dim SNe Ia, negative values for Δ and $\Delta m_{15}(B) < 1.1$ correspond to luminous SNe Ia. Histograms of the low-redshift (*solid line*) and high-redshift (*dotted line*) light curve shape parameters are mutually consistent with no indication that these samples are drawn from different populations of SNe Ia. Filled and open circles show the distribution of log (*cz*) for the low- and high-redshift samples, respectively.

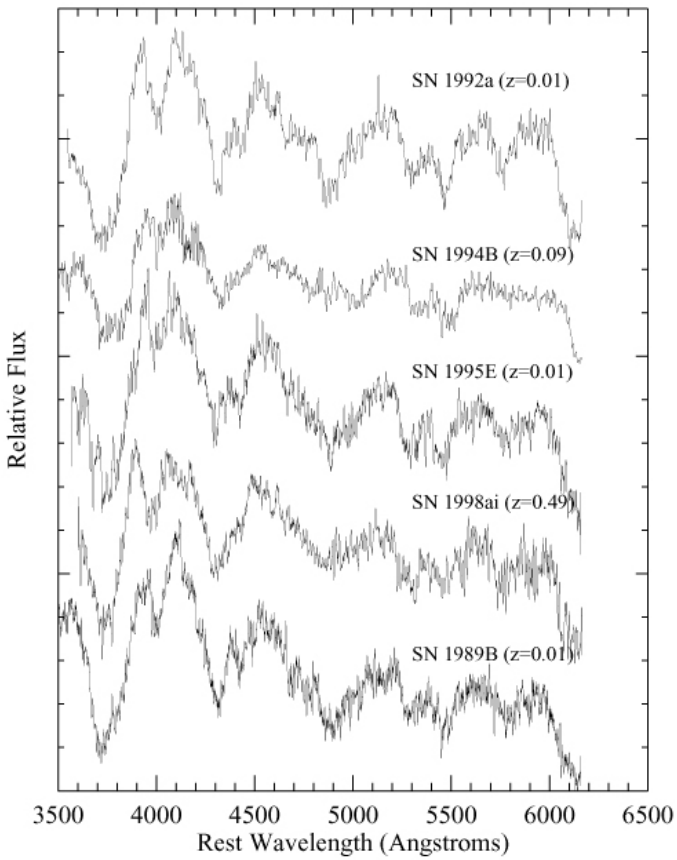

FIG. 11.—Spectral comparison (in f_λ) of SN 1998ai ($z = 0.49$) with low-redshift ($z < 0.1$) SNe Ia at a similar age. Within the narrow range of SN Ia spectral features, SN 1998ai is indistinguishable from the low-redshift SNe Ia. The spectra from top to bottom are SN 1992A, SN 1994B, SN 1995E, SN 1998ai, and SN 1989B ~5 days before maximum light. The spectra of the low-redshift SNe Ia were resampled and convolved with Gaussian noise to match the quality of the spectrum of SN 1998ai.

Sample Contamination

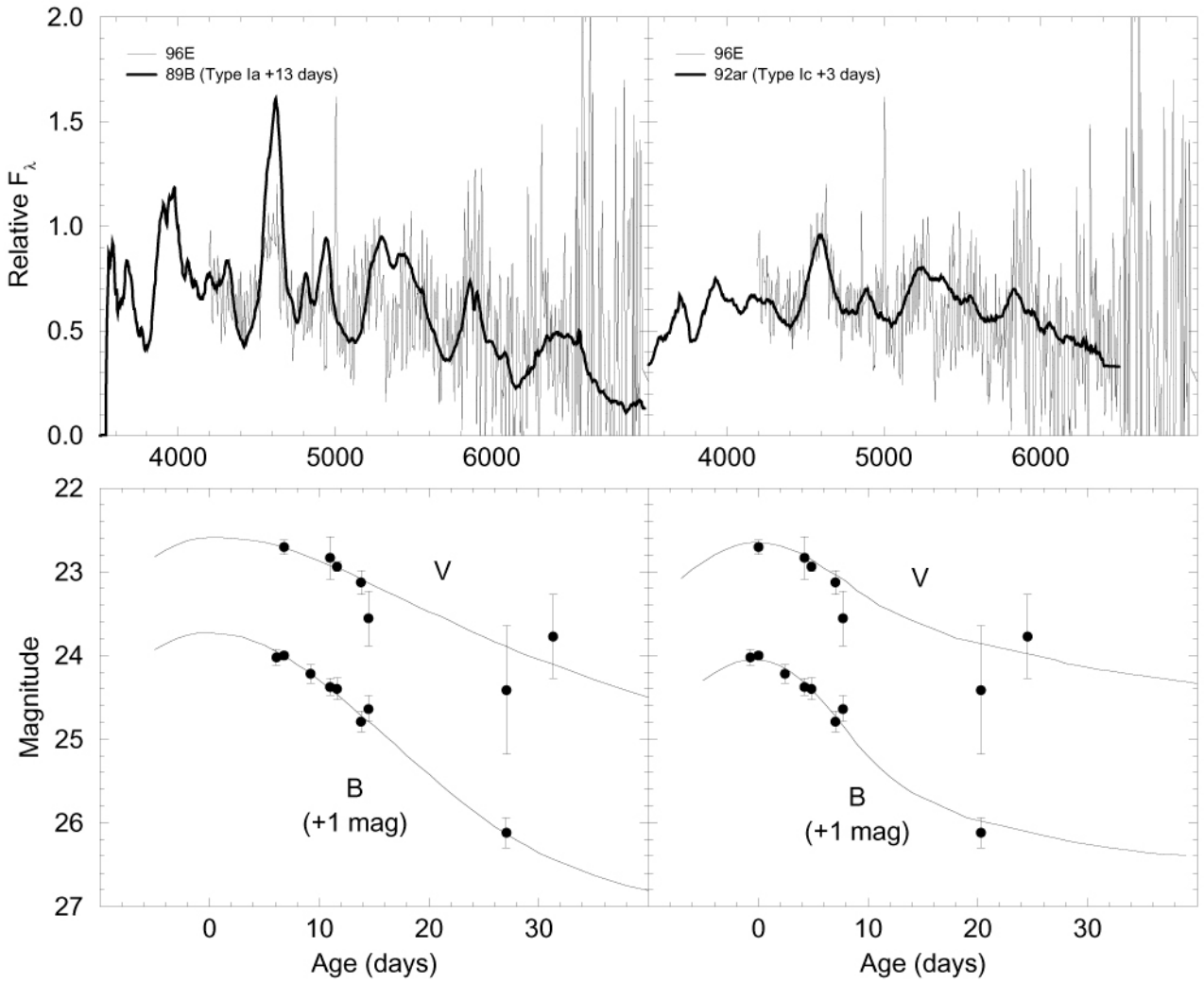

FIG. 12.—Comparison of the spectral and photometric observations of SN 1996E to those of Type Ia and Type Ic supernovae. The low signal-to-noise ratio of the spectrum of SN 1996E and the absence of data blueward of 4500 Å makes it difficult to distinguish between a Type Ia and Ic classification. The light and color curves of SN 1996E are also consistent with either supernova type. The spectrum was taken 6 days (rest frame) after the first photometric observation.